

Jens Ducreé · Thilo Brenner · Stefan Haeberle
Thomas Glatzel · Roland Zengerle

Multilamination of flows in planar networks of rotating microchannels

Received: 20 June 2005 / Accepted: 10 August 2005 / Published online: 19 October 2005
© Springer-Verlag 2005

Abstract We describe a new multilamination technique to accelerated mixing of centrifugally pumped flows through a simple network of preferentially radial, low-aspect-ratio microchannels. Mixing by multilamination is enforced by planar split-and-recombine structures, consisting of a common inlet for two concurrent centrifugal flows, and a transient region of parallel microchannels which merge again into one common outlet. A repatterning of flow is observed in each parallel channel which is induced by the Coriolis pseudo force. In a distinct regime of the parameter space spanned by the speed of rotation, the channel geometry as the viscosity (and density) of the liquids, a multilamination of flow is achieved at the entrance of the common outlet channel. We also present parallelization and cascading strategies to further enhance the homogeneity and throughput of mixing by multilamination.

1 Introduction

Centrifugal flow schemes have been deemed an elegant means to transport fluids in microfluidic systems (Burtis et al. 1972; Schembri et al. 1992; Madou and Kellogg 1998; Duffy et al. 1999; Ekstrand et al. 2000; Zeng et al. 2000a, b; Inganäs et al. 2001; Thorsén et al. 2003; Ducreé et al. 2003; Gustafsson et al. 2004; Kim et al. 2004; Puckett et al. 2004). In these devices, a disk

module is spun by a drive unit similar to conventional compact disk (CD) players or small bench-scale centrifuges. The centrifugal force provides an intrinsic means for the transport of liquid from the inlet ports near the center through designated microfluidic processing structures to the outer perimeter without a need for an external pump.

On these “lab-on-a-disk” systems, flow control is commonly achieved by the interplay of the frequency-dependent centrifugal force and passive on-disk components without moving parts. Stopping of flow during rotation is, for instance, achieved by hydrophobic patches introduced into constrictions of the channel (Zeng et al. 2000a, b; McNeely et al. 1999). These so-called capillary-burst valves block the centrifugally propelled flow below a certain frequency of rotation. In combination with an overflow channel, these valves can also provide a metering function.

However, mixing remains a major challenge in microfluidic systems. This is because the typical hydrodynamic conditions encountered in microstructures are strictly laminar, widely suppressing turbulence-formation by means of passive or even active components. The speed of mixing is therefore chiefly limited by the rate of diffusion which, in turn, scales with the characteristic dimensions of the mixing structure.

In most chip-based analytical technologies, mixing is performed in batch mode, i.e., stopped flow, in a designated reaction chamber. If mere diffusion is too slow, mixing is often accelerated by moving parts or spatially varying fields exerted on the fluid, basically mimicking the function of magnetic bar stirrer familiar from macroscopic vessels (Atencia and Beebe 2003; Ryu et al. 2004). For disk-based technologies, we have recently shown that batch mode mixing of microliter volumes can be induced by a frequent reversal of the sense of rotation, possibly in combination with the periodic deflection of paramagnetic beads by permanent magnets aligned along the orbit of the mixing chamber (Grumann et al. 2004, 2005).

Passive mixing in continuous laminar flows at low volume throughput has been realized by geometrical

J. Ducreé (✉) · R. Zengerle
HSG-IMIT, Wilhelm-Schickard-Straße 10,
78052 Villingen-Schwenningen, Germany
E-mail: jens.ducree@hsg-imit.de
Tel.: +49-761-2037476
Fax: +49-761-2037539

T. Brenner · S. Haeberle · T. Glatzel · R. Zengerle
Laboratory for MEMS Applications,
IMTEK, University of Freiburg, Georges-Köhler-Allee 106,
79110, Freiburg, Germany

surface structures (Stroock et al. 2002; Lim et al. 2003; Wang et al. 2003; Kim et al. 2004), hydrodynamic focusing (Knight et al. 1998), bended (Gelfgat et al. 2003; Howell et al. 2004) and three-dimensional channel architectures (Gelfgat et al. 2003; Liu et al. 2000; Beebe et al. 2001; Mengeaud et al. 2002; Therriault et al. 2003; Jen et al. 2003; Chen and Meiners 2004; Mingqiang and Haim 2004; Park et al. 2004), microplume injection (Miyake et al. 1993, 1997; Elwenspoek et al. 1994) and obstacles (Wang et al. 2002). In these passive structures without moving parts, the mixing energy is entirely drawn from the pumping source.

For continuous laminar flows at high volume discharge, a common scheme to reduce mixing times is the multilamination of flows, i.e., the formation of thin, alternating lamellae of liquids. Such a stratification strategy accelerates diffusive processes by reducing the diffusion length and, at the same time, by enhancing the interfacial surface area for mass transfer between the two flows. After the layers are contacted, mixing proceeds by mere diffusion between the thin lamellae without requiring transversal flow components.

Multilamination schemes are commonly realized by pressure-driven flows through three-dimensional guide structures (Branebjerg et al. 1996; Schwesinger et al. 1996; Gray et al. 1999; Hessel et al. 2003, 2004; Hardt and Schönfeld 2003; Munson and Yager 2004; Nguyen and Wu 2005; Hardt et al. 2005). To minimize the flow resistance, high-aspect ratio microchannels are required. The fabrication of these structures, combined with the need for chemically inert materials—mostly metals, so far primarily involves high-end microfabrication technologies such as UV-LIGA or even X-ray LIGA.

The aim of this paper is to present two novel methods to enhance the speed of mixing via the multilamination of centrifugally propelled flows through simple networks of rectangular microchannels in an essentially planar

(“2.5-dimensional”) geometry. The hydrodynamic operating principle roots in the Coriolis-induced secondary flow patterns (Brenner et al. 2003; Ducrée et al. 2004; Alfredsson and Persson 1989; Barua 1954; Benton 1956; Brouwers 1995, 2002) which are outlined in Sect. 1. In the subsequent Sect. 3, two new split-and-recombine concepts are introduced to enforce and scale-up a Coriolis-induced multilamination of flows. Finally in Sect. 4, we summarize the findings and give an outlook on future work.

2 Hydrodynamics in rotating channels

2.1 Forces on centrifugal flows

To understand the principle of hydrodynamic flow lamination, we examine the flow through a radial microchannel on a disk rotating at an angular frequency vector $\vec{\omega}$ (Fig. 1) (Ducrée et al. 2005). As viewed from the non-inertial frame of reference where the disk is at rest, the flow of a liquid of density ρ and viscosity η at a speed \vec{v} is exposed to two (apparent) forces: the centrifugal force (density)

$$\begin{aligned}\vec{f}_\omega &= -\rho\vec{\omega} \times (\vec{\omega} \times \vec{r}) \\ \vec{f}_\omega &= \rho r \omega^2 \hat{e}_r \quad \text{for } \angle(\vec{\omega}, \hat{e}_r) = 90^\circ\end{aligned}\quad (1)$$

points in the radial \hat{e}_r -direction to propel a parabolic velocity profile $\vec{v}(\vec{f}_\omega)$ similar to a pressure-driven flow, and the velocity-dependent Coriolis force (density)

$$\begin{aligned}\vec{f}_C &= -2\rho\vec{\omega} \times \vec{v} \\ |\vec{f}_C| &= \frac{\rho^2 \bar{r} \Delta x^2 \omega^3}{8\eta} \quad \text{for } \angle(\vec{\omega}, \vec{v}) = 90^\circ\end{aligned}\quad (2)$$

which points perpendicular to $\vec{v}(\vec{f}_\omega)$. The variable \bar{r}

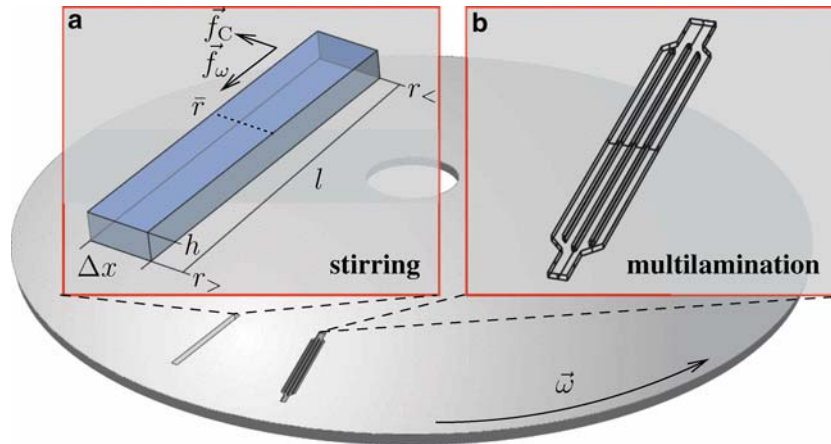


Fig. 1 Geometry and forces on a disk spinning at the angular velocity $\vec{\omega}$ pointing for positive, i.e., counter-clockwise rotation, out of the paper plane towards the reader. The rectangular channel exhibits a width Δx and height h and a mean radial position \bar{r} , pointing in the radial \hat{e}_r -direction. In the non-inertial reference

frame rotating with the disk at ω , a liquid filling a channel of length l is exposed to the centrifugal force density $\vec{f}_\omega \propto r\omega^2\hat{e}_r$ (1) and to the Coriolis force density $\vec{f}_C \propto \vec{v} \times \vec{\omega}$ (2). The plot shows a straight channel (a) where Coriolis-induced stirring occurs and a parallel channel network to implement multilamination of flow (b)

delineates the mean radial position of the liquid flow on the disk and $\angle(\vec{a}, \vec{b})$ the angle between the vectors \vec{a} and \vec{b} . The vector field \vec{f}_C peaks in the center of the channel where the parabolic centrifugal \vec{v} -profile is maximum. Note that the approximation for $|\vec{f}_C|$ in Eq. 2 has been derived by assuming a mean velocity $v = v_{\max}/2$ of a centrifugal flow with a maximum velocity $v_{\max} = \omega^2 \bar{r} \Delta x^2 / 8\eta$ through a gap of spacing Δx .

Assuming again a centrifugally driven flow through a gap of width Δx and $h \rightarrow \infty$ (Fig. 1), we retain a ratio

$$\frac{\vec{f}_\omega}{\vec{f}_C} = \frac{8\eta}{\rho \Delta x^2 \omega} \quad (3)$$

between \vec{f}_ω (1) and \vec{f}_C (2). For typical conditions of centrifugally driven flow of water ($\rho \approx 10^3 \text{ kg m}^{-3}$, $\eta \approx 1 \text{ mPa s}$) and $\Delta x = 200 \text{ }\mu\text{m}$, the ratio amounts to about $200 \omega^{-1}$, meaning that the transversal Coriolis pseudo force already supersedes the centrifugal force at rather moderate frequencies of about 32 Hz. This increasing influence of the Coriolis force towards high speeds of rotation has previously been investigated in a qualitative and quantitative fashion by simulation and experimentally verified in a flow switch based on the Coriolis force (Brenner et al. 2003, 2005).

2.2 Patterning of flow

Figure 2 sketches how the velocity field \vec{v} is shaped by the interplay of the centrifugal force \vec{f}_ω (1) and the Coriolis force \vec{f}_C (2). During rotation, a parabolic velocity profile $\vec{v}(\vec{f}_\omega)$ emerges which peaks in the center of the channel. The shape of \vec{v} is thus akin to a profile of a pressure-driven flow.

The inhomogeneous radial velocity profile $\vec{v}(\vec{f}_\omega)$ implies an inhomogeneous force field $\vec{f}_C(\vec{v})$ (2) which is (initially) directed in azimuthal direction, i.e., perpendicular to the radial channel. $\vec{f}_C(\vec{v})$ thus energizes a transversal convection from the center where \vec{f}_C is maximum towards one particular sidewall selected by the sense of rotation (Fig. 2). Continuity prescribes that the slow liquid in the outer region escapes along the outer perimeter where the field $\vec{f}_C(\vec{v})$ displays the least counterforce. The resulting transversal currents $\vec{v}(\vec{f}_C)$ lead to the “stirring” of two parallel flows.

We carried out simulations with the commercial code ACE+ (CFD-GUI Revision 2002.2.16, CFD-ACEU solver Revision 2002.0.40) from ESI Group (2000) to disclose the details. The simulations at $\omega = 300 \text{ rad s}^{-1}$ for $l = 2.1 \text{ cm}$, $\Delta x = 100 \text{ }\mu\text{m}$ and $h = 100 \text{ }\mu\text{m}$ in Fig. 3 reveal the details of the stirring under laminar conditions. An initial AB alignment in the inlet channel is transformed into a vertical ABA “sandwich” and, further downstream, into an almost entirely reversed horizontal BA like pattern. The key impact parameters governing this hydrodynamic process are the channel geometry (Δx , h , l) and the speed and sense (sign) of the rotation vector $\vec{\omega}$.

For cross-checking the simulated hydrodynamic flow patterns, we have developed an optical measurement setup to experimentally verify the patterning of flow on a centrifugal disk (Grumann et al. 2005). The setup is based on a stroboscopic principle where a top-view mounted microscope camera is triggered each given integer number of turns by the zero-crossing of the centrifuge engine. The b/w camera exhibits an extremely short minimum exposure time of 100 ns, only. To investigate an arbitrary region on the spinning disk, a linear drive moves the camera along the radial axis while a time delay adjusts the azimuthal position.

The captured gray-scale intensities are then calibrated with a set of water–ink mixtures at known mixing ratios. For each position, top-view images of concurrent water and ink flows are then compared to the accumulated intensity along a vertical line in the corresponding simulation. The so-obtained experimental data portrayed in Fig. 3 prove good qualitative and quantitative agreement with the simulation (Ducrée et al. 2004).

3 Multilamination strategies

Based on this Coriolis-induced rearrangement of flows, we designed two novel split-and-recombine schemes to implement a multilamination of flow within planar microchannel geometries. In each case, two incoming flows are first contacted in a horizontal AB-type layer. The Coriolis stirring (Fig. 3) then reverses the AB into a BA-type layer. The two concepts differ as the so-called direct laminator achieves the half-turn in a single step while the so-alternative sandwich laminator enforces two consecutive quarter turns.

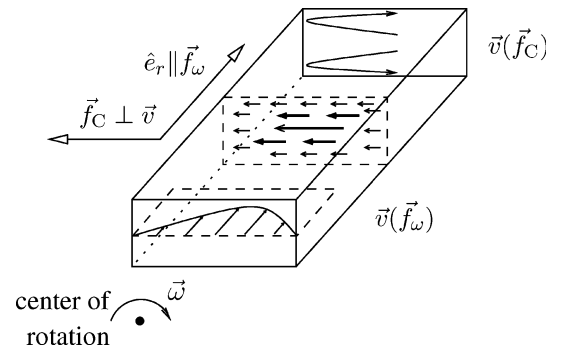


Fig. 2 Schematic of the patterning of flow in a fluidic duct spinning at an angular frequency ω . The centrifugal force (density) \vec{f}_ω (1) generates a parabolic profile \vec{v} pointing (mainly) in radial \hat{e}_r direction. The Coriolis force \vec{f}_C (2) seeks to deflect the flow in transversal direction. As the transversal motion in the filled channel is restricted by the sidewalls, the non-uniform flow field \vec{v} in a cross section of the channel leads to an inhomogeneous field distribution of the Coriolis force $\vec{f}_C(\vec{v}) \perp \vec{v}$. The field peaks in the center of the channel where the liquid is pushed toward the sidewall from where it escapes along the upper and lower sidewall. This way transversal swirling currents $\vec{v}(\vec{f}_C)$ are generated

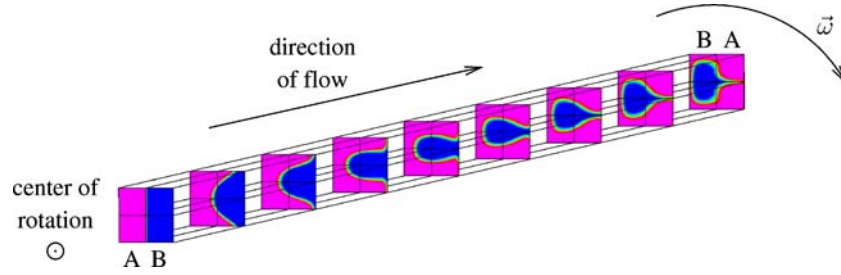


Fig. 3 Coriolis-induced hydrodynamic reversal of an horizontal AB layer in a straight radial channel. The channel which measures a width $\Delta x = 100 \mu\text{m}$ and a height $h = 100 \mu\text{m}$ extends at a length $l = 2.1 \text{ cm}$ in radial direction from its inlet at r . The speed of

rotation amount to $\omega = 50 \text{ rad s}^{-1}$ in clockwise sense. Diffusion has been suppressed in the simulation by selecting a small diffusion coefficient $D = 2 \times 10^{-20} \text{ m}^2 \text{ s}^{-1}$

3.1 Direct laminator

Two separate incoming flows are briefly contacted and then divided in three parallel channels (Fig. 4). In the central channel, the two-phase flow with fluid A in the left and fluid B in the right half is reversed from the initial AB pattern to a BA pattern by means of the Coriolis-driven advection (Fig. 3).

At the entrance of the common outlet, an ABAB stratification of the flows is accomplished to reduce the diffusion length by a factor of two and thus the mixing time by a factor of four. Towards the exit, the Coriolis-induced stirring persists which continuously elongates the interfacial surface to further enhance diffusive mixing. Figure 4 displays the full course of lateral flow patterning (at radially compressed aspect ratio) observed at $\omega = 90 \text{ rad s}^{-1}$.

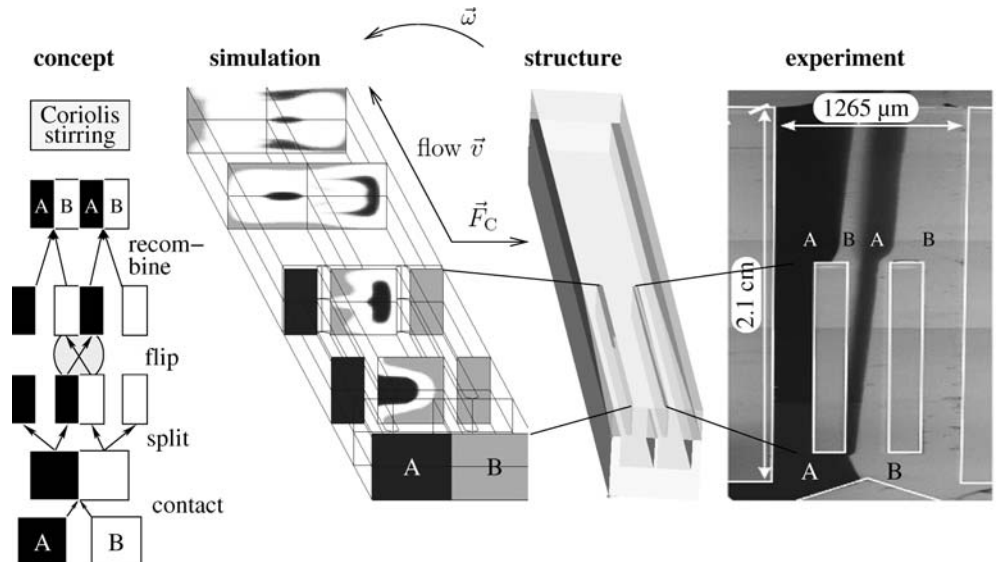
This novel split-and-recombine principle can be extended to massively reduce mixing times. By cascading a series of N (e.g., 3) congruent laminators (Fig. 5), the maximum layer thickness d (e.g., $100 \mu\text{m}$) is reduced by a factor of 2^N (8) to accelerate mixing time t_D for diffusive mixing by a factor of 2^{2N} (64)!

3.2 Sandwich laminator

The second split-and-recombine scheme achieves the half-turn after two consecutive quarter turns (Fig. 6). By slightly prolonging the common inlet channel, the first partial rotation already completes right at the point where the flows are split. Vertical BAB sandwiches then enter each parallel channel to finish the second leg of the half turn. Overall, the lamination structure has transformed the horizontal BA layering at its entrance into an ABABABAB pattern at its exit, thus reducing the mixing distance by a factor of four and the (diffusive) mixing time by a factor of $4^2 = 16$.

Note that, by referring the conceptual scheme displayed in Fig. 6 (left), this scaling of the mixing time is clearly idealized. In the simulation as well as in the experiment shown in the same Fig. 6, it can be recognized that there is a systematic asymmetry between the flow patterns in each parallel channel, tracing back to the imperfect sandwich alignment at the entrance. The authors presume that in a hydrodynamically optimized (asymmetric) geometry, the distribution of the layer widths could be significantly reduced.

Fig. 4 Direct laminator—concept, simulation, layout and experimentally observed patterning of flow. The structure features a width $\Delta x = 1265 \mu\text{m}$, a height $h = 60 \mu\text{m}$, and a length of 2.1 cm , starting at a distance r from the center of rotation in radial direction. The simulation is carried out at $\omega = 150 \text{ rad s}^{-1}$ with the same geometry



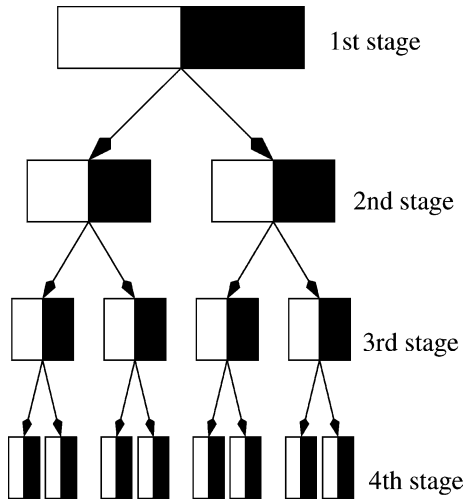


Fig. 5 Cascading scheme for the direct laminator. In each stage, the width of the parallel channels cuts into halves, thus decreasing the diffusion time by a factor of four. Due to the scaling of the flow resistance with the length and the inverse square of the channel cross section, the overall resistance increases with each additional stage, despite the increasing parallelism of the channels

3.3 Scale-up

Mixing by multilamination is of particular interest for micro process engineering where, in addition to rapid and homogeneous mixing, also the volume discharge is of outstanding importance. As low channel cross sections are imperative for fast diffusive mixing in passive microstructures, scale-up has to be accomplished numbering-up “identical” structures.

Recalling the previous multilamination principles, we discover that the sandwich laminator features a generic numbering-up strategy by increasing the number of channels branching off a common inlet. In practice, a maximum count of parallel channels is imposed by the lateral spreading the Coriolis force can induce to form the required BAB sandwich.

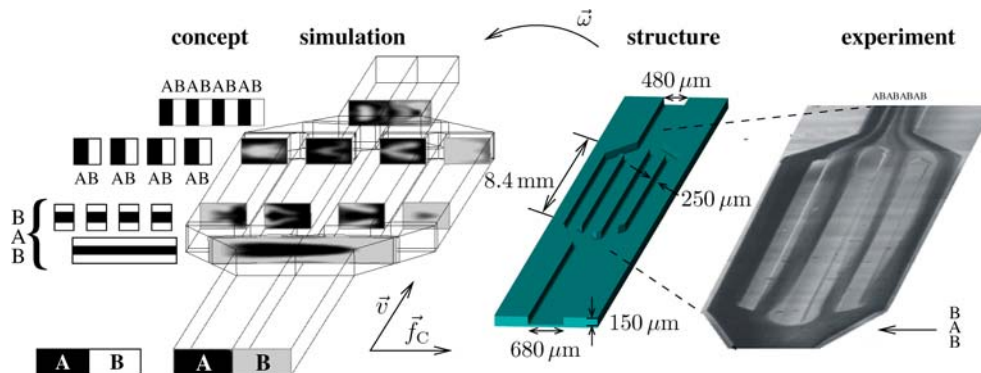


Fig. 6 Sandwich laminator—concept, simulation, layout and experimentally observed multilamination of flow at $\omega = 180 \text{ rad s}^{-1}$. A centrifugal flow is driven through a simple structure with four channels in parallel (insert). The experiment

For the direct laminator, numbering-up can be implemented by cascading congruent structures. Note, however, that this implies that the channel width has to be reduced by a factor of two in each stage of the cascade. The practical limit is then given by the minimum feature size of the manufacturing technology as well as the throttling of the overall throughput by the rapidly narrowing channel cross sections.

At first glance, the cascaded sandwich laminator thus appears to be the method of choice for scale-up by numbering-up. But the overall throughput can also be ramped up by replicating identical structures according to the rotational symmetry of the disk.

4 Summary and outlook

We have shown multilamination of concurrent centrifugal flows by split-and-recombine scheme to substantially accelerate mixing in a planar structure of rectangular, “2.5-dimensional” microchannels. Accompanying CFD simulations revealed that this novel actuation scheme is based on the apparent Coriolis force, energizing transversal advection between centrifugal flows through rotating microchannels. The key parameters impacting the Coriolis-stirring are the channel geometry, the angular velocity and the radial downstream position.

Two alternative split-and-recombine concepts, the direct laminator and the sandwich laminator, have been presented to enforce multilamination of flow. Scale-up of volume throughput by distinct numbering-up strategies have been investigated. We mention that the clean horizontal stratification achieved in Figs. 4 and 6 proves to be quite sensitive to the experimental parameters. However, a significantly enhanced “wild” mixing, i.e., a mixing without patterns which are recognizable from a top-view position, always occurs, regardless of the experimental parameters. This wild mixing just reflects

with water and ink displays an eightfold lamination in the outlet section. The course of lamination from AB at the inlet to ABABABAB can be followed in the simulation (right)

in a less pronounced or completely washed out gray profile across the channel.

In the future, we will incorporate the Coriolis-induced multilamination of flow into a Coriolis reactor where the liquid educts are continuously delivered in a free jet from stationary dispensers to cylindrical receiving reservoirs rotating with the disk (Ducrée et al. 2004; Haerberle et al. 2005). After passing the here described multilamination structures, the mixed liquids are expelled from side openings of the disk to the wall of the surrounding receiving vessel.

This Coriolis reactor platform offers several advantages. Compared to pressure driven setups, pumping is enforced pulse-free fashion by the centrifugal volume force. The contact free transmission of force without the need for pressure-tight interfaces facilitates handling of the mixing module. The mixing platform can also be supplemented with other previously introduced centrifugal microfluidic technologies such as a flow switch based on the Coriolis force (Brenner et al. 2003, 2005), beads as stationary phases (Grumann et al. 2004, 2005) and actuators (Grumann et al. 2004, 2005) as well as optical readout elements (Grumann et al. 2005).

Acknowledgements The authors are grateful to the support by the federal state of Baden–Württemberg for the grant “Bio-Disk” (No. 24-720.431-1-7/2) (Bio-Disk 2003) and the support of the CoMix project (CoMix – Coriolis Microreactor 2004) by the Landesstiftung Baden–Württemberg.

References

- Burtis CA, Mailen CJ, Johnson WF, Scott CD, Tiffany TO, Anderson NG (1972) Development of miniature fast analyzer. *Clin Chem* 18(8):753–761
- Schembri CT, Ostoich V, Lingane PJ, Burd TL, Buhl SN (1992) Portable simultaneous multiple analyte whole-blood analyzer for point-of-care testing. *Clin Chem* 38(9):1665–1670
- Madou MJ, Kellogg GJ (1998) LabCD: a centrifuge-based microfluidic platform for diagnostics. In: Cohn GE (ed) Proceedings of SPIE—Systems & Technologies for Clin. Diagn. & Drug Disc, volume 3259, pp 80–93
- Duffy DC, Gillis HL, Lin J, Sheppard NF, Kellogg GJ (1999) Microfabricated centrifugal microfluidic systems: characterization and multiple enzymatic assays. *Anal Chem* 71(20):4669–4678
- Ekstrand G, Holmquist C, Örlfors AE, Hellman B, Larsson A, Andersson P (2000) Microfluidics in a rotating CD. In: van den Berg A, Olthuis W, Bergveld P (eds) Proceedings of the micro total analysis systems symposium (μ TAS 2000) May 14–18, Enschede, The Netherlands. Kluwer, The Netherlands, pp 311–314
- Zeng J, Banerjee D, Deshpande M, Gilbert JR (2000) Design analyses of capillary burst valves in centrifugal microfluidics. In: van den Berg A, Olthuis W, Bergveld P (eds) Proceedings of the micro total analysis systems symposium (μ TAS 2000) May 14–18, Enschede, The Netherlands. Kluwer, pp 493–496
- Zeng J, Deshpande M, Greiner K, Gilbert JR (2000) Fluidic capacitance model of capillary-driven stop valves. In: ASME international mechanical engineering congress and exposition (IMECE'00)
- Inganäs M, Ekstrand G, Engström J, Eckersten A, Dérand H, Andersson P (2001) Quantitative bio-affinity assays at nanoliter scale, parallel analysis of crude protein mixtures. In: Ramsey JM, van den Berg A (eds) Proceedings of the micro total analysis systems symposium (μ TAS 2001), October 21–25, Monterey, pp 91–92
- Thorsén G, Ekstrand G, Selditz U, Wallenborg SR, Andersson P (2003) Integrated microfluidics for parallel processing of proteins in a CD microlaboratory. In: Northrup MA, Jensen KF, Harrison DJ (eds) Proceedings of the 7th international conference on micro total analysis systems (μ TAS 2003), October 5–9, Squaw Valley, volume 1 of *MESA Monographs*, Kluwer, pp 457–460
- Ducrée J, Brenner T, Glatzel T, Zengerle R (2003) A Coriolis-based split-and-recombine laminator for ultrafast mixing on rotating disks. In: Northrup MA, Jensen KF, Harrison DJ (eds) Proceedings of the 7th international conference on micro total analysis systems (μ TAS 2003), October 5–9, Squaw Valley, volume 1 of *MESA Monographs*, Kluwer, pp 603–606
- Gustafsson M, Hirschberg D, Palmberg C, Jörnvall H, Bergman T (2004) Integrated sample preparation and MALDI mass spectrometry on a microfluidic compact disk. *Anal Chem* 76(2):345–350
- Kim J, Jang SH, Jia G, Zoval JV, da Silva NA, Madou MJ (2004) Cell lysis on a microfluidic CD (compact disc). *Lab Chip* 4(5):516–522
- Puckett LG, Dikici E, Lai S, Madou M, Bachas LG, Daunert S (2004) Investigation into the applicability of the centrifugal microfluidics platform for the development of protein-ligand binding assays incorporating enhanced green fluorescent protein as a fluorescent reporter. *Anal Chem* 76(24):7263–7268
- McNeely MR, Spute MK, Tusneem NA, Oliphant AR (1999) Hydrophobic microfluidics. In: Ahn CH, Frazier AB (eds) Proceedings of SPIE—microfluidic devices and systems II, volume 3877, pp 210–220
- Atencia J, Beebe DJ (2003) An oscillating ferromagnetic micro-pump utilizing centrifugal force. In: Northrup MA, Jensen KF, Harrison DJ (eds) Proceedings of the 7th international conference on micro total analysis systems (μ TAS 2003), October 5–9, Squaw Valley, pp 883–886
- Ryu KS, Shaikh K, Goluch E, Fan Z, Liu C (2004) Micro magnetic stir-bar mixer integrated with parylene microfluidic channels. *Lab Chip* 4(6):608–613
- Grumann M, Geipel A, Riegger L, Zengerle R, Ducrée J (2004) Magneto-hydrodynamic micromixing for centrifugal lab-on-a-disk platforms. In: Laurell T, Nilsson J, Jensen KF, Harrison DJ, Kutter JP (eds) Proceedings of the 8th international conference on micro total analysis systems (μ TAS 2004), September 26–30, Malmö, Sweden, volume 1, RSC, pp 593–595
- Grumann M, Geipel A, Riegger L, Zengerle R, Ducrée J (2005) Batch-mode mixing with magnetic beads on centrifugal microfluidic platforms. *Lab Chip* 5(5):560–565
- Stroock AD, Dertinger SK, Adjari A, Mezic I, Stone HA, Whitesides GM (2002) Chaotic mixer for microchannels. *Science* 295(5555):647–651
- Lim D, Kamotani Y, Cho B, Mazumder J, Takayama S (2003) Fabrication of microfluidic mixers and artificial vasculatures using a high-brightness diode-pumped Nd:YAG laser direct write method. *Lab Chip* 3(4):318–323
- Wang H, Iovenitti P, Harvey E, Masood S (2003) Numerical investigation of mixing in microchannels with patterned grooves. *J Micromech Microeng* 13(6):801–808
- Kim DS, Lee SW, Kwon TH, Lee SS (2004) A barrier embedded chaotic micromixer. *J Micromech Microeng* 14(6):798–805
- Knight JB, Vishwanath A, Brody JP, Austin RH (1998) Hydrodynamic focusing on a silicon chip: mixing nanoliters in microseconds. *Phys Rev Lett* 80(17):3863–3866
- Gelfgat AY, Yarin AL, Bar-Yoseph PZ (2003) Dean vortices-induced enhancement of mass transfer through an interface separating two immiscible liquids. *Phys Fluid* 15(2):330–347
- Howell PB Jr, Mott DR, Golden JP, Ligler FS (2004) Design and evaluation of a Dean vortex-based micromixer. *J Micromech Microeng* 4(6):663–669

- Liu RH, Stremmer MA, Sharp KV, Olsen MG, Santiago JG, Adrian RJ, Aref H, Beebe DJ (2000) Passive mixing in a three-dimensional serpentine microchannel. *J Microelectromech Syst* 9(2):190–197
- Beebe DJ, Adrian RJ, Olsen MG, Stremmer MA, Aref H, Jo B-H (2001) Passive mixing in microchannels: fabrication and flow experiments. *Mech Ind* 2(4):343–348
- Mengeaud V, Jossierand J, Girault HH (2002) Mixing processes in a zigzag microchannel: finite element simulations and optical study. *Anal Chem* 74(16):4279–4286
- Therriault D, White SR, Lewis JA (2003) Chaotic mixing in three-dimensional microvascular networks fabricated by direct-write assembly. *Nat Mater* 2:265–271
- Jen C-P, Wu C-Y, Lin Y-C, Wub C-Y (2003) Design and simulation of the micromixer with chaotic advection in twisted microchannels. *Lab Chip* 3(2):77–81
- Chen H, Meiners J-C (2004) Topologic mixing on a microfluidic chip. *Appl Phys Lett* 84(12):2193–2195
- Mingqiang Yi, Haim HB (2004) The kinematics of bend-induced mixing in micro-conduits. *Int J Heat Fluid Flow* 24(5):645–656
- Park S-J, Kim JK, Park J, Chung S, Chung C, Chang JK (2004) Rapid three-dimensional passive rotation micromixer using the breakup process. *J Micromech Microeng* 14(1):6–14
- Miyake R, Lammerink TSJ, Elwenspoek M, Fluitman JHJ (1993) Micro mixer with fast diffusion. In: Proceedings of IEEE micro electro mechanical systems (MEMS'93), February 7–10, Fort Lauderdale, Florida, pp 248–253
- Elwenspoek M, Lammerink TSJ, Miyake R, Fluitman JHJ (1994) Towards integrated microliquid handling systems. *J Micromech Microeng* 4(4):227–245
- Miyake R, Tsuzuki K, Takagi T, Imai K (1997) A highly sensitive and small flow-type chemical analysis system with integrated absorptometric micro-flowcell. In: Proceedings of the 10th IEEE annual international workshop on micro electro mechanical systems (MEMS'97), January 26–30, Nagoya, Japan, pp 102–107
- Wang H, Iovenitti P, Harvey E, Masood S (2002) Optimizing layout of obstacles for enhanced mixing in microchannels. *Smart Mater Struct* 11(5):662–667
- Branebjerg J, Gravesen P, Krog JP (1996) Fast mixing by lamination. In: Proceedings of the 9th IEEE annual international workshop on micro electro mechanical systems (MEMS'96), February 11–15, San Diego, pp 441–446
- Schwesinger N, Frank T, Wurmus H (1996) A modular microfluid system with an integrated micromixer. *J Micromech Microeng* 6(1):99–102
- Gray BL, Jaeggi D, Mourlas NJ, van Driehuisen BP, Williams KR, Maluf NI, Kovacs GTA (1999) Novel interconnection technologies for integrated microfluidic systems. *Sensor Actuat A—Phys* 77(1):57–65
- Hessel V, Hardt S, Löwe H, Schönfeld F (2003) Laminar mixing in different interdigital micromixers: I. experimental characterization. *AIChE J* 49(3):566–577
- Hessel V, Hardt S, Löwe H (2004) Chemical micro process engineering: fundamentals, modelling and reactions. Wiley, New York
- Hardt S, Schönfeld F (2003) Laminar mixing in different interdigital micromixers: II. numerical simulations. *AIChE J* 49(3):578–584
- Munson MS, Yager P (2004) Simple quantitative optical method for monitoring the extent of mixing applied to a novel microfluidic mixer. *Anal Chim Acta* 507(1):63–71
- Nguyen N-T, Wu Z (2005) Micromixers—a review. *J Micromech Microeng* 15(2):R1–R16
- Hardt S, Drese KS, Hessel V, Schönfeld F (2005) Passive micromixers for applications in the microreactor and μ TAS fields. *Microfluidic Nanofluidic*
- Brenner T, Zengerle R, Ducrée J (2003) A flow-switch based on Coriolis force. In: Northrup MA, Jensen KF, Harrison DJ (eds) Proceedings of the 7th international conference on micro total analysis systems (μ TAS 2003), October 5–9, Squaw Valley, volume 2 of MESA Monographs, Kluwer, pp 903–906
- Ducrée J, Schlosser P, Glatzel T, Zengerle R (2004) Centrifugal platform for high-throughput reactive micromixing. In: Laurell T, Nilsson J, Jensen KF, Harrison DJ, Kutter JP (eds) Proceedings of the 8th international conference on micro total analysis systems (μ TAS 2004), September 26–30, Malmö, Sweden, volume 1, RSC, pp 554–556
- Alfredsson PH, Persson H (1989) Instabilities in channel flow with system rotation. *J Fluid Mech* 202:543–557
- Barua SN (1954) Secondary flow in a rotating straight pipe. *Proc Roy Soc A* 227:133–139
- Benton GS (1956) The effect of the earth's rotation on laminar flow in pipes. *J Appl Mech* 23:123–127
- Brouwers JH (1995) Secondary flow and particle centrifugation in slightly tilted rotating pipes. *Appl Sci Res—Now Flow Turbu Combust* 55:95–105
- Brouwers JH (2002) Phase separation in centrifugal fields with emphasis on the rotational separator. *Int J Exp Heat Trans Thermodynam Fluid Mech* 26:325–334
- Ducrée J, Haerberle S, Brenner T, Glatzel T, Zengerle R (2005) Patterning of flow and mixing in rotating radial microchannels. *Microfluidic Nanofluidic*, 2005, status: accepted on 2005-05-05
- Brenner T, Glatzel T, Zengerle R, Ducrée J (2005) Frequency-dependent transversal flow control in centrifugal microfluidics. *Lab Chip* 5(2):146–150
- ESI Group—CFD—ACE+ (2000) http://www.esi-group.com/SimulationSoftware/CFD_ACE/
- Grumann M, Brenner T, Beer C, Zengerle R, Ducrée J (2005) Visualization of flow patterning in high-speed centrifugal microfluidics. *Rev Sci Instru* 76(2):025101
- Haerberle S, Brenner T, Schlosser H-P, Zengerle R, Ducrée J (2005) Centrifugal micromixer. *Chem Eng Technol* 28(5):613–616
- Grumann M, Dobmeier M, Schippers P, Brenner T, Kuhn C, Fritsche M, Zengerle R, Ducrée J (2004) Aggregation of bead-monolayers in flat microfluidic chambers—simulation by the model of porous media. *Lab Chip* 4(3):209–213
- Grumann M, Riegger L, Nann T, Ehlert O, Mittenbühler K, Urban G, Pastewka L, Brenner T, Zengerle R, Ducrée J (2005) Parallelization of chip-based fluorescence immunoassays with quantum-dot labelled beads. In: Proceedings of the 13th international conference on solid-state sensors, actuators and microsystems (Transducers'05), June 5–9, Seoul, Korea, volume 2, pp 1114–1117
- Grumann M, Moser I, Kohn C, Urban G, Riegger L, Steigert J, Zengerle R, Ducrée J (2005) Optical beam guidance in monolithic polymer chips for miniaturized colorimetric assays. In: Proceedings of the 18th IEEE international conference on micro electro mechanical systems (MEMS'05), January 30–February 3, Miami, pp 108–111
- Bio-Disk project (2003) <http://www.bio-disk.com>, June 2003
- CoMix—Coriolis Microreactor project (2004) <http://www.coriolis-microreactor.com>, December 2004